Low-temperature spin dynamics of doped manganites: Roles of Mn t_{2g}, Mn e_g, and O $2p$ states

Priya Mahadevan
JRCAT-Angstrom Technology Partnership, 1-1-4 Higashi, Tsukuba, Ibaraki 305-0046, Japan

I. V. Solovyev
JRCAT-Angstrom Technology Partnership, 1-1-4 Higashi, Tsukuba, Ibaraki 305-0046, Japan
and Institute of Metal Physics, Russian Academy of Sciences, Ekaterinburg GSP-170, Russia

K. Terakura
JRCAT-NAIR, 1-1-4 Higashi, Tsukuba, Ibaraki 305-8562, Japan
and Institute of Industrial Science, University of Tokyo, 7-22-1 Roppongi, Minato-ku, Tokyo 106-8558, Japan
(Received 26 April 1999)

The low-temperature spin dynamics of doped manganites have been analyzed within a tight-binding model, the parameters of which are estimated by mapping the results of *ab initio* density-functional calculations onto the model. This approach is found to provide a good description of the spin dynamics of the doped manganites, observed earlier within the *ab initio* calculations. Our analysis not only provides some insight into the roles of the e_g and the t_{2g} states but also indicates that the oxygen p states play an important role in the spin dynamics. This may cast doubt on the adaptability of the conventional model Hamiltonian approaches to the analysis of spin dynamics of doped manganites. [S0163-1829(99)06839-3]

There has been resurgence of interest in transition-metal oxides with the perovskite structure owing to their wide range of electronic and magnetic properties. Among them, the hole-doped manganites[1] have been occupying a special position: they exhibit dramatic phenomena like colossal magnetoresistance and are being intensively studied with prospect for technological applications. $LaMnO_3$, the parent material of the manganites, is an antiferromagnetic insulator. Upon sufficient doping ($x \sim 0.15$) with divalent ions (such as Sr, Ca), the system is driven metallic. The holes are allowed to move only if adjacent spins are parallel, which results in a dramatic increase in the conductivity when the spins order ferromagnetically, an effect that can be induced by applying a magnetic field or by lowering the temperature below the Curie temperature T_c. Thus, the carrier mobility is intimately related to the underlying magnetic state of the system, and there have been considerable efforts in recent times to identify the interactions that control the magnetoresistive properties. An approach in this direction has been to analyze the spin dynamics of the doped manganites.

Early experiments on $La_{0.7}Pb_{0.3}MnO_3$ (Ref. 2) indicated that the spin-wave dispersion $\omega(\mathbf{q})$ in the doped manganites could be interpreted in terms of a conventional Heisenberg ferromagnet with only the nearest-neighbor exchange coupling. This behavior is consistent with the double-exchange limit of the one-band ferromagnetic Kondo lattice model,[3] implying that conduction e_g electrons move in a tight-binding band with one orbital per site and interact with localized t_{2g} spins via the large intra-atomic exchange J_H. However, more recent experiments[4] on other doped manganites have found strong deviation of $\omega(\mathbf{q})$ from the simple cosinelike behavior expected from a nearest-neighbor Heisenberg model. Farther-neighbor interactions in addition to the nearest-neighbor one had to be taken into account to reproduce softening of the dispersions for the wave vector $\mathbf{q}$ approaching the zone boundary. The one-band models could not explain the observed zone-boundary softening, even qualitatively.[3,5] It was then suggested that additional degrees of freedom, probably the lattice degrees of freedom, may play an important role in the spin dynamics of these materials. Recently,[6] it was shown that the softening at the zone boundary has a purely electronic origin, and could be explained within the framework of *ab initio* density-functional band calculations, in the local-spin-density approximation (LSDA).

The previous work[6] also carried out a perturbative analysis of the exchange interaction strengths within a tight-binding model considering the double degeneracy of e_g levels on the Mn site. It was argued that the degeneracy of e_g orbitals plays important roles, and simply by taking into account the proper structure of the kinetic hopping between nearest-neighbor e_g levels one can, to a large extent, understand the behavior of two strongest interactions, J_1 and J_4, in the half-metallic regime. Here, J_k corresponds to the exchange interaction between the kth neighbor atoms,[7] as defined later by Eq. (2). Furthermore, it was pointed out that a realistic model including the oxygen p orbitals and the Mn t_{2g} orbitals could indeed modify the quantitative aspects of the results. While the fully filled majority-spin t_{2g} orbitals could contribute an antiferromagnetic superexchange component to J_1, the partially filled minority spin t_{2g} orbitals could, as suggested by the *ab initio* band structure calculations, contribute a ferromagnetic double-exchange component. Further, J_2 was found to increase quite strongly in the e_g-only model, unlike the weak dependence seen in the *ab initio* results. The previous work[6] suggested that the oxygen p bands could modify J_2 considerably as the Mn $3d$-O $2p$ energy separation is comparable with the exchange splitting of the majority- and minority-spin orbitals. In the light of these observations, we have attempted to make further quan-

titative analysis to understand the origin of the observed zone-boundary softening. This has been done by mapping the results of the *ab initio* band structure calculations onto a tight-binding model that gives us flexibility of constructing simpler models and analyzing the contributions to the observed softening.

The band structure for hypothetical cubic ferromagnetic $LaMnO_3$ with the lattice parameter of 3.934 Å, calculated within the linear-muffin-tin orbital method with the atomic sphere approximation (LMTO-ASA), was mapped onto a nearest-neighbor tight-binding model[8] that had been found to give a good description of the electronic structure of the transition-metal oxides of the form $LaMO_3$, where M = Ti-Ni. The tight-binding Hamiltonian consists of the bare energies of the transition metal d (ϵ_d) and the oxygen p (ϵ_p) states and hopping interactions between the orbitals on neighboring atoms. The nearest-neighbor hopping interactions were expressed in terms of the four Slater-Koster parameters, namely $pp\sigma$, $pp\pi$, $pd\sigma$, and $pd\pi$. Note that no direct d-d hopping was taken into account. While p-d covalency effects lift the degeneracy of the d orbitals, an additional interaction $sd\sigma$ between the transition metal d and oxygen $2s$ orbitals was required to lift the degeneracy at the Γ point.[9] The energy of the oxygen $2s$ level was fixed at -20 eV. In order to obtain the magnetic ground state within the single-particle tight-binding model, we have introduced an extra parameter (ϵ_{pol}) that is the bare energy difference between the up- and down-spin d electrons at the same site. An additional splitting, (ϵ'_{pol}) was introduced between the up- and down-spin d orbitals of e_g symmetry.[10] The parameters entering the tight-binding Hamiltonian were determined by the least-squares fitting of the energies obtained from tight-binding calculations at several k points to those obtained from the LMTO calculations. It should be noted that the deep-lying oxygen $2s$ bands were not involved in the fitting. The extracted parameters are $sd\sigma=-1.57$ eV, $pp\sigma=0.91$ eV, $pp\pi=-0.23$ eV, $pd\sigma=-2.02$ eV, $pd\pi=1.0$ eV, $\epsilon_d-\epsilon_p=0.48$ eV, $\epsilon_{pol}=3.2$ eV, and $\epsilon'_{pol}=0.3$ eV being consistent with the earlier estimate for the system.[8]

The frozen spin spiral approximation,[11] where the orientation of the magnetic moment at each atomic site is spirally modulated by the wave vector $\mathbf{q}$, was used to calculate the exchange interaction $J_{\mathbf{q}}$ defined by

$$J_{\mathbf{q}}=\sum_k J_k \exp[i\mathbf{q}\cdot\mathbf{R}_k], \tag{1}$$

where $\mathbf{R}_i$ is the position vector of ith Mn atom. J_k is the kth neighbor exchange interaction appearing in the Heisenberg Hamiltonian given by

$$E[\{\mathbf{e}_i\}]=-\frac{1}{2}\sum_{ik} J_k \mathbf{e}_i\cdot\mathbf{e}_{i+k}, \tag{2}$$

with $\mathbf{e}_i$ denoting the direction of the magnetic moment at the site i. By using the local force theorem,[12] the changes in the single-particle energy could be related to the exchange interaction by mapping onto the Heisenberg model as defined above. A rigid band picture was adopted to simulate the doping effects.[13] Simplified models were constructed to elucidate the mechanism of zone-boundary softening of the spin wave, and comparison was made with the results from the LMTO calculations whenever possible to ensure that the present result is not an artifact of a particular parameter set.

In Fig. 1(a) we show the LMTO results for the spin dispersion $\omega(\mathbf{q};x)$ along the symmetry directions ΓX, XM, and MR calculated for several doping values x. In the small $\mathbf{q}$ region, the spin excitations have a weak dependence on doping as is evident from the result along the ΓX direction. However, sufficiently away from the Γ point, the results become a strong function of the concentration x. Considering the result for $x=0.4$ along the ΓX direction, we see that the spin dispersion is almost flat from midway to the zone boundary. The experimental result for $Pr_{0.63}Sr_{0.37}MnO_3$ (Ref. 4) along ΓX shows very similar behavior. The results of the tight-binding model, calculated by using the parameters extracted by fitting the *ab initio* band structure are shown in Fig. 1(b). This model calculation is called model *A* in order to distinguish from other models discussed later. Model *A* is seen to provide a good description of the energetics of the spin dynamics observed within the *ab initio* approach. The results in Fig. 1 suggest that the difference in energy between the ferromagnetic ground state and the various commensurate antiferromagnetic (AF) spin configurations such as those defined at the X (A-type AF), M (C-type AF), and R (G-type AF) points decreases with doping.

The Fourier transform of $J_{\mathbf{q}}$ gives us the real space exchange integrals J_i as shown in Fig. 2. Dominant interactions are all confined within the linear -Mn-O-Mn-$\cdots$ chains parallel to $\langle 001\rangle$ as was pointed out already.[6] They are J_i with $i=1$, 4, and 8. J_2 is the interaction for the pairs along $\langle 110\rangle$ and takes relatively small values partly because of the cancellation between the contribution from the Mn d bands and that from O p states. These results are consistent with the analysis of the experimental results[4] that required finite J_4 and J_8 to be included in the Heisenberg Hamiltonian in order to reproduce the experimentally observed spin-wave dispersions. In order to understand the behavior of the spin-wave dispersion $\omega(\mathbf{q};x)$ in terms of J_i, the following expressions for $\mathbf{q}\|x$ will be useful.

$$\hbar\omega(q_x)\simeq 2[(J_1+4J_2)\sin^2\tfrac{1}{2}q_x a + J_4\sin^2 q_x a + J_8\sin^2\tfrac{3}{2}q_x a], \tag{3}$$

where a is the lattice constant of the cubic unit cell. For $q_x a\ll 1$, the above expression reduces to

$$\hbar\omega(q_x)\simeq\tfrac{1}{2}[J_1+4J_2+4J_4+9J_8](q_x a)^2, \tag{4}$$

which helps us understand the weak dependence of the low-energy excitations on the concentration x. The large prefactors for J_4 and J_8 indicate that modest changes in J_4 and J_8 are sufficient to offset the large changes in J_1 found within our model. At the X point, Eq. (3) reduces to

$$\hbar\omega\left(q_x=\frac{\pi}{a}\right)\simeq 2J_1+8J_2+2J_8. \tag{5}$$

As the dependence of J_2 on x is weak, the changes at the zone boundary are driven by J_1 and J_8. Unlike in the low q regime, the prefactors of J_1 and J_8 are equal in this case.

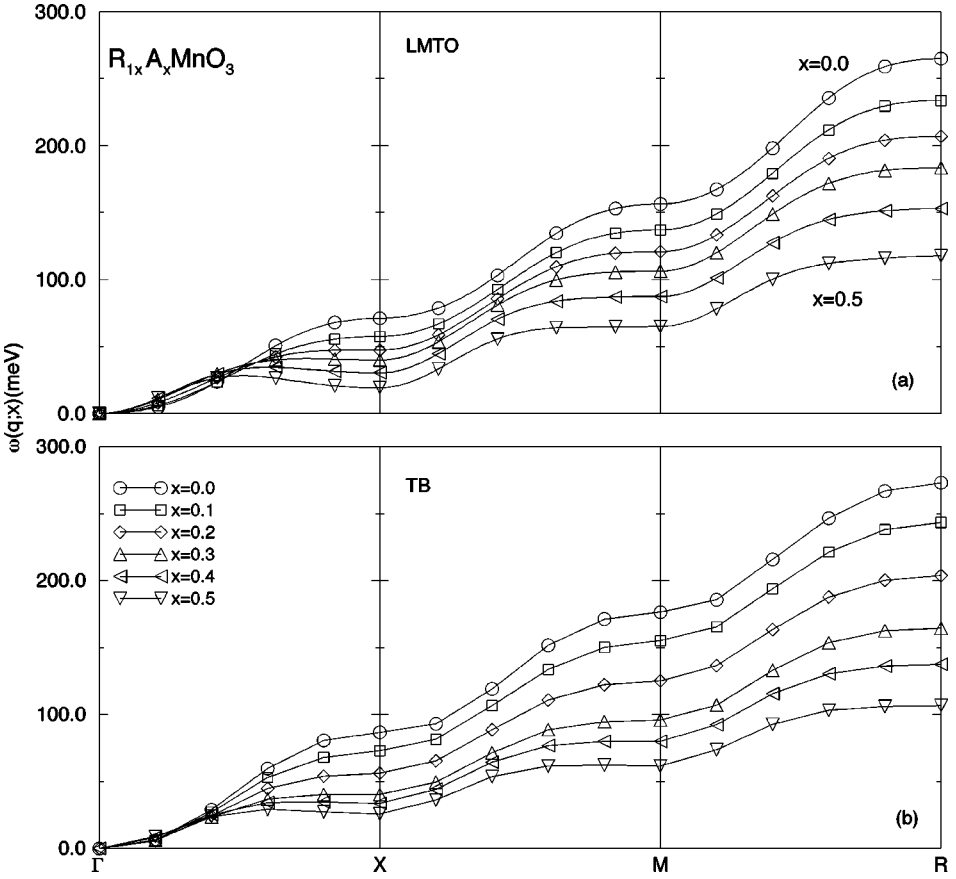

FIG. 1. The spin-wave dispersions obtained by (a) LMTO calculations and (b) the tight-binding approach (model A) along the symmetry directions ΓX, XM, and MR shown as a function of doping.

Since the decrease in J_1 is much larger than the increase in J_8, the energy at the X point decreases as the hole concentration is increased. Another useful information about the flattening of the dispersion beyond half way to the zone boundary is given by comparing Eq. (5) with

$$\hbar\omega\left(q_x=\frac{\pi}{2a}\right)\simeq J_1+4J_2+2J_4+J_8. \tag{6}$$

The energies at $q_x=\pi/a$ and $q_x=\pi/2a$ are comparable when $J_1\sim 2J_4$.

We constructed simpler models to make quantitative estimates for the contribution from the t_{2g} electrons and that from the e_g electrons. Model $B(C)$ includes e_g (t_{2g}) orbitals on the Mn atoms and all p orbitals on the oxygens. As the density of states (DOS) obtained within model A suggests partial occupancy of the minority spin t_{2g} bands with ~ 0.175 electrons even for the undoped case, the Fermi energy (E_F) of model C in the undoped case was adjusted so that the minority-spin t_{2g} bands had 0.175 electrons. As a consequence, the number of holes in the majority-spin e_g states of model B in the undoped case should be larger by 0.175 than the case when the minority-spin t_{2g} states are not occupied. The d partial DOS for models B and C along with the result for model A, which considers all d orbitals on the Mn atom, are shown in Fig. 3. The reduced models (B and C) are found to give a good description of the respective d partial DOS of e_g and t_{2g} symmetry within model A. Further justification for the treatment of the contributions from e_g and t_{2g} states separately is given by the fact that the dominant contributions, (J_i, $i=1,4,8$), are all for the pairs along $\langle 100\rangle$ for which there is no mixing of the two states in the exchange coupling. The spin-wave dispersion was calculated in the reduced models separately. The dispersion along the ΓX direction for model B is shown in the panel b [inset of Fig. 3(a)]. y denotes the number of doped e_g holes with

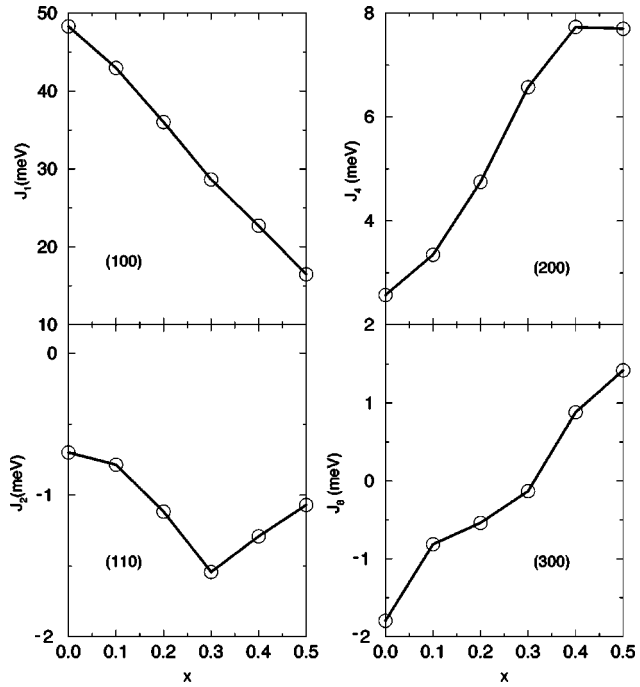

FIG. 2. The doping dependence of the exchange couplings J_1, J_2, J_4, and J_8 between atoms at (a 0 0), (a a 0), ($2a$ 0 0), and ($3a$ 0 0), where a is the lattice parameter.

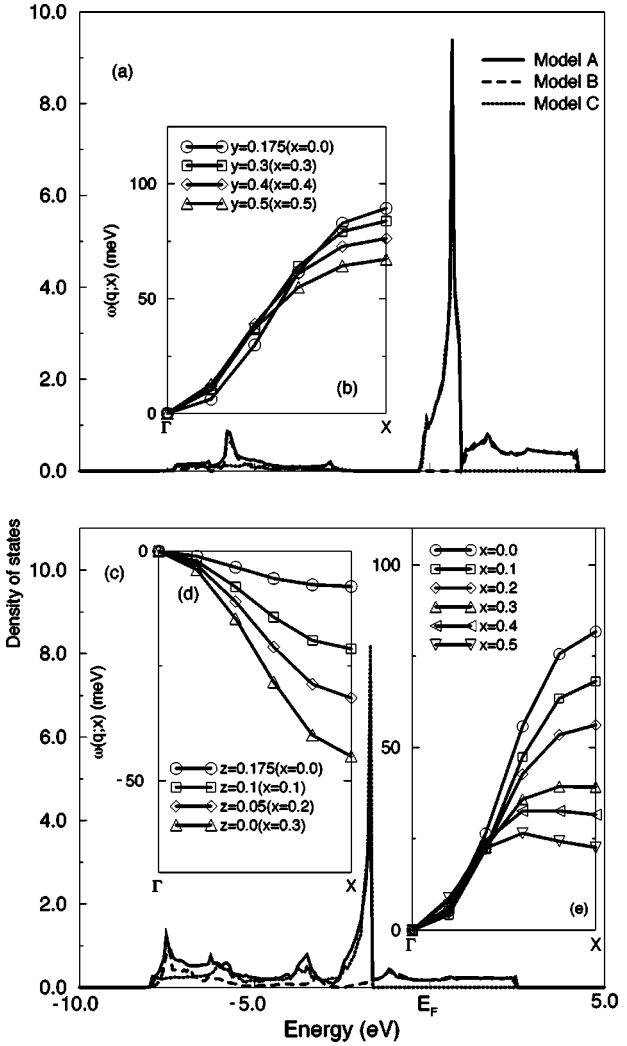

FIG. 3. The (a) minority-spin and (c) majority-spin d partial density of states within models A, B, and C. The spin-wave dispersions along ΓX as a function of doping within models (b) B and (d) C are shown along with (e) the combined contributions of models B and C. y refers to the hole concentration in the majority-spin e_g band with reference to its half-filled case. z is the electron concentration in the minority-spin t_{2g} band. x is the net concentration of the doped holes and is given by $x=y-z$.

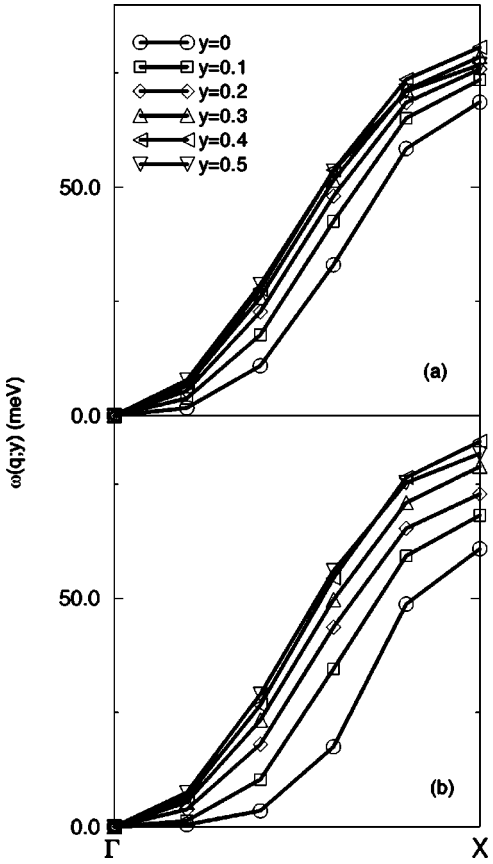

FIG. 4. The dependence of the spin-wave energies on the e_g hole doping y along ΓX within model D. The hopping between oxygen atoms and the t_{2g} orbitals on the Mn atom have been left out of the model. (a) $pd\sigma=-2.02$ eV and (b) $pd\sigma=-2.25$ eV.

reference to the half-filled majority-spin e_g band. (Equivalently, $1-y$ is the number of electrons in the e_g band.) x in the parentheses indicates the hole concentration in model A being equivalent to doping of divalent atoms. By considering the above situation, $y=0.175$ corresponds to the case of undoped $LaMnO_3$, i.e., $x=0$. As the number of holes increases from $y=0.175$, the spin-wave energy at the X point steadily decreases. In model C, on the other hand, the dominant contribution from the t_{2g} states to the exchange coupling is antiferromagnetic superexchange. The negative spin-wave energy for all q [Fig. 3(d)] is consistent with this expectation. However, small occupation of the minority spin t_{2g} states produces a ferromagnetic double-exchange contribution. z in Fig. 3(d) denotes the number of electrons in the minority-spin t_{2g} states. Clearly, doping of divalent elements reduces z so that the double-exchange contribution diminishes rapidly as is clearly seen in the z dependence of the spin-wave dispersion in Fig. 3(d). Here again the corresponding value of x in model A are indicated in brackets. The contribution from the e_g states [Fig. 3(b)] and that from the t_{2g} states [Fig. 3(d)] for the common x value are added and the resultant spin-wave dispersion shown in Fig. 3(e) agrees very well with the one in Fig. 1(b) (model A). This analysis suggests that the main source of the zone-boundary softening of the spin-wave dispersion by doping of divalent atoms for $x<0.3$ is the reduction in the ferromagnetic double exchange of the t_{2g} electrons. On the other hand, in the doping range of $x>0.3$, the t_{2g} states may simply act as a source of antiferromagnetic superexchange and further softening and flattening of the spin-wave dispersion comes from the e_g states.

The doped holes within our model have considerable oxygen p character, and the earlier results[6] suggested that the itinerant oxygen band could modify the various exchange interaction strengths. It was pointed out that the role of oxygen p states in the superexchange interaction is not only to mediate the d-d transfer but also to make a direct additional contribution.[14,15] However, in this treatment the banding effect of oxygen p states was neglected. This assumption will not be justified for quantitative arguments if the p band width is comparable to the p-d energy separation, which is the case in our systems. In order to obtain information about the role of the oxygen p band, we made further simplification in the model B that the hopping between oxygen atoms was neglected, i.e., $pp\sigma=pp\pi=0$ (model D). As the neglect of the hopping between the oxygen atoms could reduce the e_g bandwidth, the spin-wave dispersions were calculated for

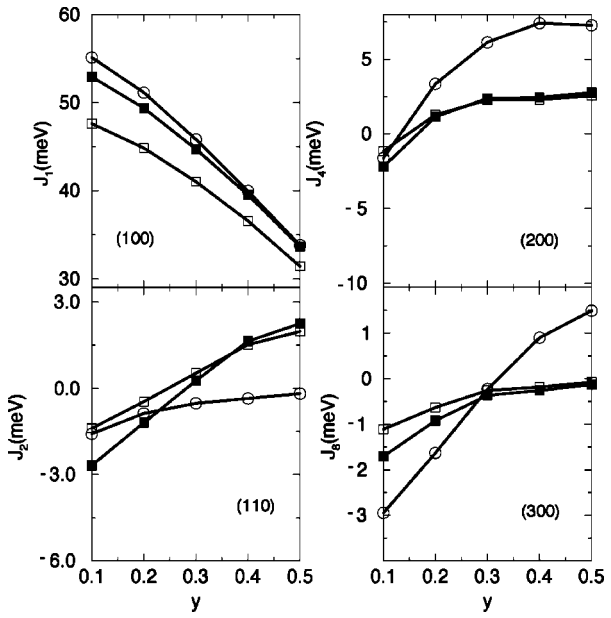

FIG. 5. The variation of the exchange couplings J_1, J_2, J_4, and J_8 with the e_g hole doping y. Open circles are for the case (model B) including the hopping between oxygen atoms and $pd\sigma = -2.02$ eV. Open and filled squares are for the cases (model D) without the hopping between oxygen atoms: $pd\sigma = -2.02$ eV (open squares) and $pd\sigma = -2.25$ eV (filled squares). The t_{2g} orbitals on the Mn atom have been left out of the basis set.

two values of $pd\sigma$—the value (-2.02 eV) estimated already by the fitting [results are shown in Fig. 4(a)] and an increased value of -2.25 eV [results are shown in Fig. 4(b)]. The dispersions shown in Figs. 4(a) and 4(b) are qualitatively similar to each other. In both cases, the spin-wave energy at the X point increases with doping being in contradiction to the behavior observed in Fig. 1 and Fig. 3(b). Since this model does not take into account the antiferromagnetic superexchange contributions coming from the t_{2g} degrees of freedom and affecting primarily the nearest-neighbor magnetic interactions, the ferromagnetic coupling J_1 remains to be the strongest interaction in the system. In such a situation, the form of the spin-wave dispersion is close to the cosinelike.

To analyze further the role played by the interoxygen hopping, the exchange interactions $\{J_i\}$ were obtained for the cases corresponding to Fig. 3(b) and Fig. 4. The results are shown in Fig. 5. As is expected, the behavior of J_1 is not affected so much by the p-p hopping. By comparing the results of model A in Fig. 2 with those of model B in Fig. 5, we see that the doping dependence of J_4 and J_8 comes primarily from the e_g electrons. Neglect of the p-p hopping (model D) strongly suppresses J_4 and J_8 for $x \geqslant 0.2$, and zone-boundary softening of the spin-wave dispersion become less pronounced. On the other hand, increase of J_2 with hole doping is enhanced by neglecting the p-p hopping. The energy at X point increases in Fig. 4 (model D) with hole doping, because the variation in J_1 in this case is not enough to offset the sharp increase in J_2.

In summary, we have analyzed the low-temperature spin dynamics of the doped manganites with tight-binding models. Our results provide some insight into the roles of the t_{2g} and the e_g states and also suggest that the channel of hopping between the oxygen atoms strongly modifies the exchange interactions. Thus for the correct quantitative and sometimes even qualitative description, the simplifications made by model Hamiltonian approaches that consider only the e_g orbitals are questionable.

We thank Professor D.D. Sarma for useful discussions. Part of the programs used here were developed in Professor Sarma's group. The present work was partly supported by NEDO.

[1] R. von Helmolt, J. Wecker, B. Holzaphel, L. Schultz, and K. Samwer, Phys. Rev. Lett. **71**, 2331 (1993); A. Asamitsu, Y. Moritomo, Y. Tomioka, T. Arima, and Y. Tokura, Nature (London) **373**, 407 (1995).

[2] T. G. Perring, G. Aeppli, S. M. Hayden, S. A. Carter, J. P. Remeika, and S. W. Cheong, Phys. Rev. Lett. **77**, 711 (1996).

[3] V. Yu. Irkhin and M. I. Katsnelson, Zh. Éksp. Teor. Fiz. **88**, 522 (1985) [Sov. Phys. JETP **61**, 306 (1985)]; N. Furukawa, J. Phys. Soc. Jpn. **65**, 1174 (1996).

[4] H. Y. Hwang, P. Dai, S. W.Cheong, G. Aeppli, D. A. Tennant, and H. A. Mook, Phys. Rev. Lett. **80**, 1316 (1998).

[5] J. Zang, H. Röder, A. R. Bishop, and S. A. Trugman, J. Phys.: Condens. Matter **9**, L157 (1997); T. K. Kaplan and S. D. Mahanti, *ibid.* **9**, L291 (1997); J. Loos and H. Fehske, Physica B **259-261**, 801 (1999).

[6] I. V. Solovyev and K. Terakura, Phys. Rev. Lett. **82**, 2959 (1999).

[7] J_1, J_2, J_3, J_4, and J_8 are the interactions in the cubic lattice corresponding to the interatomic vectors $[0,0,a]$, $[a,a,0]$, $[a,a,a]$, $[0,0,2a]$, and $[0,0,3a]$, where a is the cubic lattice constant.

[8] Priya Mahadevan, N. Shanthi, and D. D. Sarma, Phys. Rev. B **54** 11 199 (1996); Priya Mahadevan, N. Shanthi, and D. D. Sarma, J. Phys.: Condens. Matter **9**, 3129 (1997).

[9] L. F. Mattheiss, Phys. Rev. B **2**, 3918 (1970).

[10] The parameter ϵ'_{pol} is anyway small and turns out not to be important in the following calculations.

[11] L. M. Sandratskii, Phys. Status Solidi B **135**, 167 (1986); Adv. Phys. **47**, 91 (1998).

[12] A. I. Liechtenstein, M. I. Katnelson, V. P. Antropov, and V. A. Gubanov, J. Magn. Magn. Mater. **67**, 65 (1987), and references therein; I. V. Solovyev and K. Terakura, Phys. Rev. B **58**, 15 496 (1998).

[13] I.e., we start with the undoped cubic ferromagnetic $LaMnO_3$, whose electronic structure has been obtained self-consistently, and shift the position of the Fermi level in order to adjust the required hole concentration x, without an additional self-consistency. Note that this is different from the procedure used in Ref. 6, where the electronic structure of the hypothetical virtual-crystal alloy was calculated self-consistently in the framework of LSDA for each concentration x.

[14] T. Oguchi, K. Terakura, and A. R. Williams, Phys. Rev. B **28**, 6443 (1983).

[15] J. Zaanen and G. A. Sawatzky, Can. J. Phys. **65**, 1262 (1987).